

Position Controller Synthesis for The Redundant Hydraulic Shoulder Manipulator

H. Sadjadian[†] and H. D. Taghirad

Advanced Robotics and Automated Systems (ARAS)

Department of Electrical Engineering

K.N. Toosi University of Technology

[†]Sadjadian@alborz.kntu.ac.ir

Abstract – In this paper, position control has been designed for a 3 DOF actuator redundant spherical parallel manipulator. A two norm minimization approach has been used to resolve the actuator redundancy problem. Robust stability of the closed loop system is analyzed considering uncertainties inherent in the dynamic model of the manipulator. A simulation study is also performed to show the effectiveness of the proposed method. The results show the applicability of simple and conventional controllers to control redundant spherical parallel manipulators.

Index Terms – Parallel manipulator, Robust Position Control, Redundancy, Force Distribution, Computed Torque.

I. INTRODUCTION

Manipulator control has been the subject of research in the field of robotics for many years. The highly nonlinear dynamics of manipulator which includes several factors such as inertia, Coriolis and Centrifugal effects, gravity or friction has always been one of the challenging issues in the manipulator control problem.

Different classifications have been made in the literature for the manipulator controllers. An important category which distinct the main goal of the controller is position vs. force control schemes. Position control was addressed in the 1970 s to develop control schemes capable of controlling a manipulator's motion in its workspace. These strategies were found to be inadequate in performing tasks involving interaction with the environment which led to force control schemes. A large number of control techniques have been developed and used in the last three decades performing either position or force control most of which consider conventional series or non-redundant manipulators. The extension of robotics applications to new areas such as space, underwater and micro-robotics and parallel and redundant manipulation has brought new challenges in robotics research [1].

In recent years, parallel link manipulators have been among the most considerable research topics in the field of robotics. A parallel manipulator typically consists of a moving platform that is connected to a fixed base by several limbs. The number of limbs is at least equal to the number of degrees of freedom (DOF) of the moving platform so that each limb is driven by no more than one actuator, and all actuators can be mounted on or near the fixed base. These

robots are now used in real-life applications such as force sensing robots, fine positioning devices, and medical applications [2,3].

Comparing to serial robots, parallel manipulators have shown to satisfy the same structure and properties in the dynamic equation. Therefore, the vast control literature developed for serial manipulators can be extended to this class of manipulators [7]. However, the dynamics of redundant parallel manipulators is much more complicated compared even to common non-redundant parallel manipulators.

Parallel manipulators with 3 DOF have been also implemented for applications where 6 DOF are not required, such as high-speed machine tools. Recently, 3 DOF parallel manipulators with more than three limbs have been investigated, in which the additional limbs separate the function of actuation from that of constraints at the cost of increased mechanical complexity [5]. Although redundant parallel manipulators have been investigated to some extent like in [7,8,9], development of control schemes that could make use of specific properties of these structures such as managing the extra degrees of actuation has not received much attention so far and is still regarded as an interesting problem in parallel robotics research particularly for spherical or spatial parallel manipulators.

In this paper, position control of a 3-DOF redundant parallel manipulator has been considered in detail. Importance of solving the redundancy problem has been highlighted in a computed-torque redundant position control structure. Effects of uncertainties in the dynamic model are also discussed leading to a robust control structure for the manipulator. The paper is organized as follows: Section 2 contains the mechanism description, while kinematics modeling of the mechanism is reviewed in section 3. In section 4 dynamic formulation of the manipulator is discussed in brief as a key element in model based control design. The proposed structure for position control of the manipulator is elaborated in section 5 which is followed by a detail robust analysis in section 6. Finally, the results are analyzed using a simulation study.

II. MECHANISM DESCRIPTION

A schematic of the mechanism, which is currently under experimental studies in ARAS Robotics Lab, is

shown in Fig. 1. The mechanism is originally designed by Vincent Hayward [10], borrowing design ideas from biological manipulators particularly the biological shoulder. The interesting features of this mechanism and its similarity to human shoulder have made its design unique, which can serve as the basis for a good experimental setup for parallel robot research. As shown in figure 1, the mobile platform is constrained to spherical motions. Four high performance hydraulic piston actuators are used to give three degrees of freedom in the mobile platform. Each actuator includes a position sensor of LVDT type and an embedded Hall Effect force sensor. The four limbs share an identical kinematic structure. A passive limb connects the fixed base to the moving platform by a spherical joint, which suppresses the pure translations of the moving platform. Simple elements like spherical and universal joints are used in the structure. A complete analysis of such a careful design will provide us with required characteristics regarding the structure itself, its performance, and the control algorithms.

From the structural point of view, the shoulder mechanism which, from now on, we call it "the Hydraulic Shoulder" falls into an important class of robotic mechanisms called parallel robots. The orientation angles are limited to vary between $-\pi/6$ and $\pi/6$. No sensors are available for measuring the orientation angles of the moving platform which justifies the importance of the forward kinematic map as a key element in feedback position control of the shoulder with the LVDT position sensors used as the output of such a control scheme. In former studies by the authors, different numerical approaches have been used to solve the forward kinematic map of this manipulator [11]. Furthermore, complete kinematic modeling resulting in a closed-form forward kinematics solution, Jacobian analysis through a complete velocity analysis of the mechanism, and singularity analysis are all discussed in detail in [12]. Also, closed-form dynamic model has been performed in [13] as a basis for model-based position control schemes.

III. HYDRAULIC SHOULDER KINEMATICS

Fig. 2 depicts a geometric model for the hydraulic shoulder manipulator which will be used for its kinematics derivation. Two coordinate frames are defined for the purpose of analysis. The base coordinate frame $\{A\}: x_0y_0z_0$ is attached to the fixed base at point C (rotation center) with its z_0 -axis perpendicular to the plane defined by the actuator base points $A_1A_2A_3A_4$ and an x_0 -axis parallel to the bisector of angle $\angle A_1CA_4$. The second coordinate frame $\{B\}: x_1y_1z_1$ is attached to the center of the moving platform P with its z -axis perpendicular to the line defined by the actuators moving end points (P_1P_2) along the passive limb. Note that we have assumed that the actuator fixed endpoints lie on the same plane as the rotation center C.

The position of the moving platform center P is defined by:

$${}^A p = [p_x, p_y, p_z]^T \quad (1)$$

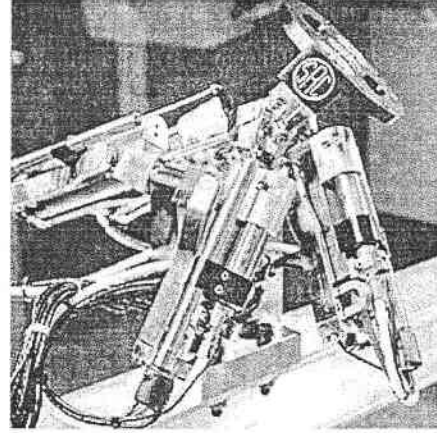


Figure 1. The Hydraulic Shoulder Manipulator

Also, a rotation matrix ${}^A R_B$ is used to define the orientation of the moving platform with respect to the base frame:

$${}^A R_B = R_z(\theta_z)R_y(\theta_y)R_x(\theta_x)$$

$$= \begin{bmatrix} c\theta_x c\theta_y & c\theta_x s\theta_y s\theta_z - s\theta_x c\theta_z & c\theta_x s\theta_y c\theta_z + s\theta_x s\theta_z \\ s\theta_x c\theta_y & s\theta_x s\theta_y s\theta_z + c\theta_x c\theta_z & s\theta_x s\theta_y c\theta_z - c\theta_x s\theta_z \\ -s\theta_y & c\theta_y s\theta_z & c\theta_y c\theta_z \end{bmatrix} \quad (2)$$

where $\theta_x, \theta_y, \theta_z$ are the orientation angles of the moving platform denoting rotations of the moving frame about the fixed $x, y,$ and z axes respectively. Also $c\theta$ and $s\theta$ denote $\cos(\theta)$ and $\sin(\theta)$ respectively. With the above definitions, the 4×4 transformation matrix ${}^A T_B$ is easily found to be:

$${}^A T_B = \begin{bmatrix} {}^A R_B & {}^A p \\ \mathbf{0} & 1 \end{bmatrix} \quad (3)$$

Hence, the position and orientation of the moving platform are completely defined by six variables, from which, only three orientation angles $\theta_x, \theta_y, \theta_z$ are independently specified as the task space variables of the hydraulic shoulder.

The kinematic vector-loop equation for each actuated limb can be written as:

$$L_i = l_i s_i = {}^A p + {}^A R_B {}^B p_i - a_i \quad (4)$$

where l_i is the length of the i^{th} actuated limb and s_i is a unit vector pointing along the direction of the i^{th} actuated limb. Also, ${}^A p$ is the position vector of the moving platform and ${}^A R_B$ is its rotation matrix. Vectors a_i and ${}^B p_i$ denote the fixed end points of the actuators (A_i) in the base frame and their moving end points respectively, written as:

$$\begin{aligned} a_1 &= {}^A A_1 = (l_b \sin \alpha \quad -l_b \cos \alpha \quad 0)^T, \\ a_2 &= {}^A A_2 = (-l_b \sin \alpha \quad -l_b \cos \alpha \quad 0)^T, \\ a_3 &= {}^A A_3 = (-l_b \sin \alpha \quad l_b \cos \alpha \quad 0)^T, \\ a_4 &= {}^A A_4 = (l_b \sin \alpha \quad l_b \cos \alpha \quad 0)^T, \end{aligned} \quad (5)$$

and,

$$\begin{aligned} {}^B p_1 &= (0 \quad -l_d \quad -l_k)^T, \\ {}^B p_2 &= (0 \quad l_d \quad -l_k)^T. \end{aligned} \quad (6)$$

Hence, the actuator lengths l_i can be easily computed by dot-multiplying (4) with itself to yield:

$$L_i^T \cdot L_i = l_i^2 = [{}^A p + {}^A R_b^B p_i - a_i]^T [{}^A p + {}^A R_b^B p_i - a_i] \quad (7)$$

Writing (7) four times with the corresponding parameters given in (2), (5) and (6), and through algebraic simplifying, we obtain the complete kinematic model of the hydraulic shoulder [12].

For the Jacobian analysis of the Hydraulic shoulder, we must find a relationship between the angular velocity of the moving platform, ω , and the vector of limb rates as the actuator space variables, $\dot{l} = [\dot{l}_1 \ \dot{l}_2 \ \dot{l}_3 \ \dot{l}_4]^T$, so that:

$$\dot{l} = J\omega \quad (8)$$

From the above definition, it is easily observed that the Jacobian for the Hydraulic shoulder will be a 4×3 rectangular matrix as expected, regarding the mechanism as an actuator redundant manipulator. The details of the expression of the Jacobians can be found in [12].

IV. HYDRAULIC SHOULDER DYNAMICS

In this section the dynamic model of the hydraulic shoulder is derived based on the application of the Lagrange formulation with θ chosen as the vector of generalized coordinates. The equation of motion can be written as:

$$\frac{d}{dt} \left(\frac{\partial L}{\partial \dot{\theta}} \right) - \frac{\partial L}{\partial \theta} = \tau_g \quad (9)$$

where the Lagrangian function $L = T - U$ is the difference between the kinetic energy T and the potential U of the system and τ_g is the vector of the generalized torques. The kinetic energy can be written by adding translational and rotational contributions as:

$$T = T(\theta, \dot{\theta}) = \frac{1}{2} \dot{\theta}^T M(\theta) \dot{\theta} \quad (10)$$

where $\theta \in R^3$ and $M \in R^{3 \times 3}$. Similarly, the potential energy can be written as:

$$U = U(\theta) \quad (11)$$

Hence, the Lagrange equations of motion can be rewritten as:

$$\frac{d}{dt} \left(\frac{\partial T(\theta, \dot{\theta})}{\partial \dot{\theta}} \right) - \frac{\partial T(\theta, \dot{\theta})}{\partial \theta} + \frac{\partial U(\theta)}{\partial \theta} = \tau_g \quad (12)$$

Using (12), the complete dynamic model of the hydraulic shoulder can be obtained as:

$$M(\theta)\ddot{\theta} + V(\theta, \dot{\theta}) + G(\theta) = \tau - \tau_e \quad (13)$$

Where the vectors $\theta, \dot{\theta}, \ddot{\theta}$ are the moving platform orientation angle, angular velocity and angular acceleration respectively, $M(\theta)$ is the 3×3 symmetric positive definite inertia matrix, $V(\theta, \dot{\theta})$ is the 3×1 vector of Coriolis and centrifugal torques, $G(\theta)$ is the 3×1 vector of gravitational torques, τ is the 3×1 vector of moving platform torques and τ_e is the 3×1 vector of external torques applied to the moving platform. Note that the control inputs to the dynamic

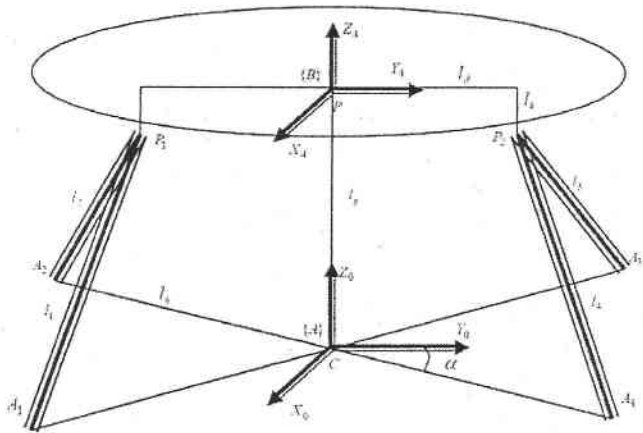


Figure 2. Geometric model for the hydraulic shoulder

equation is in fact the 4×1 vector of actuator forces, F , which is related to the moving platform torques, τ , by:

$$\tau = J^T(\theta) \cdot F \quad (14)$$

Where $J(\theta)$ is the 4×3 Jacobian matrix representing the relationship between the angular velocity of the moving platform and the vector of limb rates. The inertia Matrix $M(\theta)$ is directly given by the expression of the kinetic energy $T(\theta, \dot{\theta})$. The gravity term is obtained from the potential energy $U(\theta)$ by:

$$G(\theta) = \frac{\partial U(\theta)}{\partial \theta} \quad (15)$$

Finally, $V(\theta, \dot{\theta})$ which characterizes the Coriolis and centrifugal torques can be computed from the elements of the inertia matrix using the Christoffel symbols of the first type. More details with this respect can be found in former studies by the authors [13].

V. POSITION CONTROL

A. Problem Definition

In position control of the hydraulic shoulder the moving platform is supposed to follow a desired trajectory and the actuator forces required to produce such a motion are computed. Let $\theta_d(t)$ be the desired trajectory of the end-effector orientation angles. Also recall F as the vector of actuator forces and θ as the Cartesian coordinate variables of the hydraulic shoulder. The vector of limb's lengths l can be measured directly using limb position sensors. Regarding the fact that no measuring device is available for the orientation of the moving platform, also having a closed form forward kinematics map [12], either of the general position control topologies using inverse or forward kinematic maps could be used.

B. Inverse Dynamic Control Formulation

The inverse dynamics of the hydraulic shoulder can be written as following:

$$F = (J^T)^* [M(\theta)\ddot{\theta} + V(\theta, \dot{\theta}) + G(\theta)] \quad (16)$$

Where $(J^T)^*$ is the pseudo-inverse of the transposed Jacobian matrix of the hydraulic shoulder. This solution is perhaps the most common among all possible solutions to the inverse dynamics of the hydraulic shoulder. It is, in fact, the minimum two norm solution to a constrained optimization problem with the static equation (14) as its equality constraint which minimizes the internal forces of the shoulder manipulator. It should be noted that other possible solutions could be chosen for the actuator redundancy problem to minimize other physical performance criteria as well as choosing possible null space forces to accomplish a secondary task such as active stiffness control while the robot is tracking the reference trajectory. Details of the solution procedure to the force distribution problem with different choices of objective functions could be found in [13]. Rewriting (16) we obtain:

$$F = F_1 + F_2 = (J^T)^* [M(\theta)\ddot{\theta}] + (J^T)^* [V(\theta, \dot{\theta}) + G(\theta)] \quad (17)$$

Equation (17) suggests using F_2 as a linearizing control and F_1 in conjunction with a linear controller. In this technique, which is mostly known as the computed-torque method, full inverse dynamics is used to linearize the dynamic equations supposing perfect knowledge of the dynamic model. The linear controller will then guarantee the desired performance requirements.

Hence, the inverse dynamic control law could be written as:

$$F = (J^T)^* M(\theta)[\ddot{\theta}_d + K_p e + K_v \dot{e}] + (J^T)^* [V(\theta, \dot{\theta}) + G(\theta)] \quad (18)$$

Where e is the tracking error of the manipulator and K_p and K_v are diagonal position and velocity gain matrices.

VI. ROBUSTNESS ANALYSIS

In this section, the stability of the closed loop system under the computed torque control law is analyzed regarding the uncertainties in the dynamic model of the hydraulic shoulder. More precisely, the choices of M_0, N_0, K_p and K_v will be obtained in terms of the bounding functions of the unknown dynamics to achieve robust stability.

Usually the control law given in (17) is modified in order to consider the uncertainties inherent in the dynamic terms. In fact, the control law must depend only on the known parts of the dynamics.

Let:

$$\begin{aligned} M &= M_0 + \Delta M \\ N &= V + G = N_0 + \Delta N \end{aligned} \quad (19)$$

where M_0 and N_0 are the nominal known parts of the inertia and nonlinear effects due to the Coriolis and Centrifugal terms respectively and $\Delta M, \Delta N$ represent the corresponding uncertainties in each term. The control law could be rewritten as follows:

$$\tau = J^T F = M_0(\ddot{\theta}_d + K_p e + K_v \dot{e}) + N_0 \quad (20)$$

Using the definitions in (19), the dynamic equation can be simplified as:

$$\tau = J^T F = M(\theta)\ddot{\theta} + N(\theta, \dot{\theta}) \quad (21)$$

Combining (20) and (21) we obtain:

$$M(\theta)\ddot{\theta} + N(\theta, \dot{\theta}) = M_0(\ddot{\theta}_d + K_p e + K_v \dot{e}) + N_0 \quad (22)$$

Now by defining:

$$x = [e \quad \dot{e}]^T \quad (23)$$

We obtain:

$$\dot{x} = Ax + B\eta \quad (24)$$

Where

$$A = \begin{bmatrix} 0 & I_n \\ -M^{-1}M_0K_p & -M^{-1}M_0K_v \end{bmatrix} \quad (25)$$

$$B = \begin{bmatrix} 0 \\ M^{-1} \end{bmatrix} \quad (26)$$

And:

$$\eta = \Delta M \ddot{\theta}_d + \Delta N \quad (27)$$

Moreover, the following inequalities hold for the dynamic terms taking uncertainties into consideration [14,15]:

$$m_l I \leq M(\theta) \leq m_u I$$

$$\|N(\theta, \dot{\theta})\| \leq a_0 + a_1 \|x\| + a_2 \|x\|^2 \quad (28)$$

$$\|V(\theta, \dot{\theta})\| \leq a_3 + a_4 \|x\|$$

Where $m_l, m_u, a_0, a_1, a_2, a_3, a_4$ are some positive constants and $\|\cdot\|$ represents the Euclidean norm. Robust stability of the error system could now be proved using a direct Lyapunov approach.

Consider:

$$V(x) = x^T P x \quad (29)$$

With:

$$P = \frac{1}{2} \begin{bmatrix} kI_n + \alpha^2 M(\theta) & \alpha M(\theta) \\ \alpha M(\theta) & M(\theta) \end{bmatrix} \quad (30)$$

And:

$$k = k_p + \alpha k_v \quad (31)$$

It can be easily verified that the Lyapunov candidate will be positive definite if $k, \alpha > 0$. Furthermore, the uniform lower and upper bounds of $V(x)$ can be obtained by computing the eigenvalues of P such that:

$$\lambda_l \|x\|^2 \leq V(x) \leq \lambda_u \|x\|^2 \quad (32)$$

Where:

$$\lambda_l = \frac{m_l k}{k + m_u(1 + \alpha^2)} \quad (33)$$

$$\lambda_u = k + m_u(1 + \alpha^2)$$

Now taking the derivative of (29) we have:

$$\dot{V}(x) = x^T (A^T P + P A + \dot{P}) x + 2x^T P B \eta \quad (34)$$

Noting that:

$$y^T M y = 2y^T V_m y \quad (35)$$

We can simplify equation (34) as:

$$\dot{V}(x) = -x^T Q x + \frac{1}{2} x^T \begin{bmatrix} \alpha I_n \\ I_n \end{bmatrix} (V_m + V_m^T) [\alpha I_n \quad I_n] x + \quad (36)$$

$$\frac{1}{2} x^T \begin{bmatrix} 0 & \alpha^2 I_n \\ \alpha^2 I_n & \alpha I_n \end{bmatrix} \begin{bmatrix} M & 0 \\ 0 & M \end{bmatrix} x + x^T \begin{bmatrix} \alpha I_n \\ I_n \end{bmatrix} \eta$$

With:

$$Q = \begin{bmatrix} \alpha k_p I_n & 0 \\ 0 & k_v I_n \end{bmatrix} \quad (37)$$

Which can be bounded as follows:

$$\dot{V}(x) \leq -\lambda_1(Q) \|x\|^2 + \sqrt{1+\alpha^2} \|V_n\| \|x\|^2 + \quad (38)$$

$$\frac{1}{2} \alpha (1 + \sqrt{1+\alpha^2}) m_n \|x\|^2 + \sqrt{1+\alpha^2} \|x\| \|\eta\|$$

Where:

$$\lambda_1(Q) = \text{Min}\{\alpha k_p, k_v\} \quad (39)$$

Using the above equations, we finally obtain:

$$\dot{V}(x) \leq \|x\| (\gamma_0 - \gamma_1 \|x\| + \gamma_2 \|x\|^2) \quad (40)$$

Where:

$$\gamma_0 = \sqrt{1+\alpha^2} (a_0 + m_n \sup(\theta_d))$$

$$\gamma_1 = \lambda_1(Q) - \sqrt{1+\alpha^2} (a_1 + a_3) - \frac{1}{2} \alpha (1 + \sqrt{1+\alpha^2}) m_n \quad (41)$$

$$\gamma_2 = \sqrt{1+\alpha^2} (a_2 + a_4)$$

The following theorem gives the robust stability conditions of the error system (24) based on the derived results:

Theorem: The error system (24) is robust against bounded uncertain dynamics if:

$$\begin{aligned} M_0 K_p &= k_p I_n, \\ M_0 K_v &= k_v I_n \end{aligned} \quad (42)$$

and the positive scalar gains k_p, k_v are chosen to be large enough.

Proof: According to the derived bounds on the proposed Lyapunov function and its derivative as in (32) and (40), and using the Lemma in [14], the error system is uniformly ultimately bounded with respect to $B(0, d)$ with:

$$d = \frac{2\gamma_0}{\gamma_1 + \sqrt{\gamma_1^2 - 4\gamma_0\gamma_2}} \sqrt{\frac{\lambda_u}{\lambda_l}} \quad (43)$$

Provided that:

$$\gamma_1 > 2\sqrt{\gamma_0\gamma_2}$$

$$\gamma_1^2 + \gamma_1 \sqrt{\gamma_1^2 - 4\gamma_0\gamma_2} > 2\gamma_0\gamma_2 \left(1 + \sqrt{\frac{\lambda_u}{\lambda_l}}\right) \quad (44)$$

$$\gamma_1 + \sqrt{\gamma_1^2 - 4\gamma_0\gamma_2} > 2\gamma_2 \|x_0\| \sqrt{\frac{\lambda_u}{\lambda_l}}$$

The above conditions are met by increasing the gains k_p, k_v resulting in an increase in γ_1 .

VII. SIMULATION RESULTS

In order to verify the performance of the proposed method, a simulation study is performed. A sample trajectory was considered in the reachable workspace of the manipulator

and the proposed control law was tested along such a trajectory. Figures (3)-(4) show the tracking performance of the proposed control law along the given trajectory for the moving platform and the legs respectively. The control gains have been chosen such that the stability criteria are met. Furthermore, the moving platform tracking error is depicted in Figure (5).

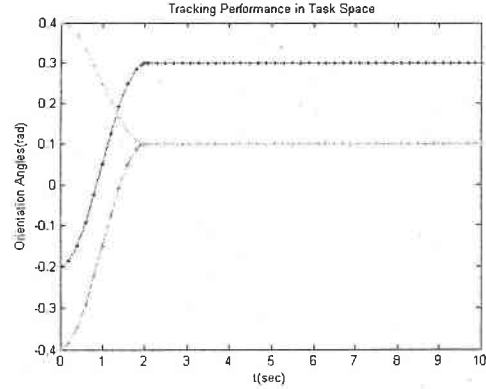


Figure 3. Tracking performance of the moving platform

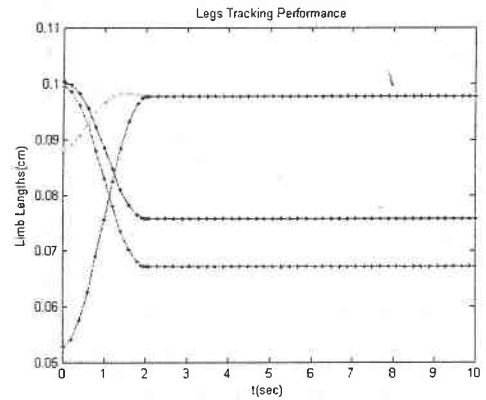


Figure 4. Tracking performance of the Legs

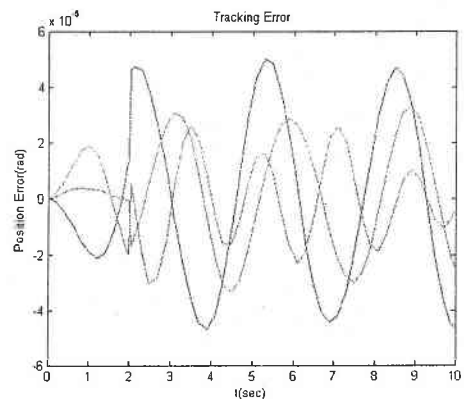


Figure 5. Tracking Error for the moving platform

It should be noted that in general the derived stability conditions usually lead to conservative gains which may affect the performance of the system regarding problems such as actuator saturation. Finally, the proposed control law was compared to a simple PD control with the same

control gains. Figures (6)-(7) show the corresponding results compared to the robust inverse dynamics control. It is obvious that the proposed inverse dynamics controller outperforms the linear controller in tracking the desired trajectory.

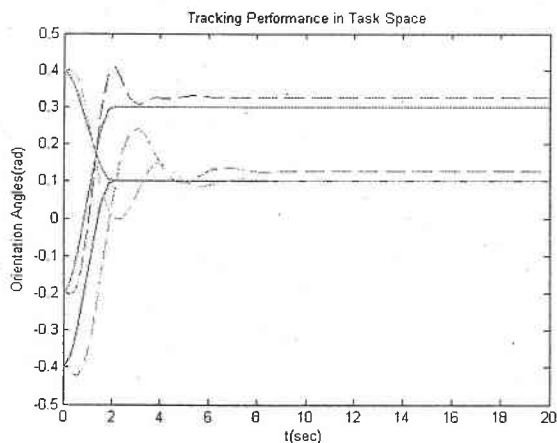


Figure 6. Moving platform tracking performance-PD control

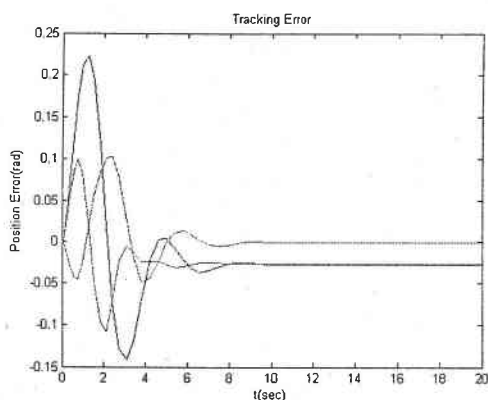


Figure 7. Tracking Error for the moving platform-PD control

VII. CONCLUSIONS

In this paper, position control has been developed for a 3-DOF actuator redundant hydraulic shoulder manipulator. The importance of a proper method for resolving the force distribution problem has been also discussed. The controller is simply of the computed torque type. The results are shown to be superior to a simple linear controller of PD type. Robustness analysis and simulation has been done in order to evaluate the application of conventional methods to control redundant spherical manipulators with a parallel structure which seem to be promising for further research in this field.

REFERENCES

[1] R.V. Patel and F. Shadpey, Control of redundant robot manipulators, theory and experiments, Springer-Verlag, 2005.
[2] J.P. Merlet, Still a long way to go on the road for

parallel mechanisms, ASME 2002 DETC Conference, Montreal, Canada, 2002.

[3] J.P. Merlet, Parallel Robots: Open problems, In 9th Int'l. Symp. of Robotics Research, Snowbird, 9-12 October 1999.
[4] Yu-Wen Li; Jin-Song Wang; Li-Ping Wang; Xin-Jun Liu, Inverse dynamics and simulation of a 3-DOF spatial parallel manipulator, IEEE International Conference on Robotics and Automation, Volume 3, 2003, 4092 - 4097.
[5] S. Joshi and L.W. Tsai, A comparison study of two 3-DOF parallel manipulators: One with three and the other with four supporting limbs, IEEE Trans. On Robotics & Automation, vol. 19, No. 2, April 2003, 200-209.
[6] Y.K. Yiu and Z.X.Li, PID and adaptive robust control of a 2-DOF over-actuated parallel manipulator for tracking different trajectory, Proc. IEEE Int'l Symposium on computational intelligence in robotics and automation, Kobe, Japan, 2003. 1052-1057.
[7] Hui Cheng, et.al., Dynamics and control of redundantly actuated parallel manipulators, IEEE/ASME Transactions on Mechatronics, vol. 8, No. 4, Dec. 2003, 483-491.
[8] H. Cheng, et.al., Advantages and Dynamics of parallel manipulators with redundant actuation, Proc. IEEE/RSJ Int'l Conference on intelligent robots and systems, USA, Nov. 2001. 171-176.
[9] A. Muller, Internal preload control of redundantly actuated parallel manipulators- Backlash avoiding control. Proc. IEEE ICRA 2005, Barcelona, Spain, April 2005, 960-965.
[10] V.Hayward, Design of a hydraulic robot shoulder based on a combinatorial mechanism, Experimental Robotics III: The 3rd Int'l Symposium, Japan Oct. 1994. Lecture Notes in Control & Information Sciences, Springer-Verlag, 297-310.
[11] H. Sadjadian and H.D. Taghirad, Comparison of Different Methods for Computing the Forward Kinematics of a Redundant Parallel Manipulator, Journal of Intelligent and Robotic Systems, Springer-Verlag, Nov 2005.
[12] H. Sadjadian and H.D. Taghirad, Kinematic, Singularity and Stiffness Analysis of the Hydraulic Shoulder: A 3-DOF Redundant Parallel Manipulator, Advanced Robotics, Vol. 20, No.7, 2006, 763-781.
[13] H. Sadjadian, Kinematic, Dynamic Modeling and Position Control of the Hydraulic Shoulder Manipulator with proper force distribution, Ph.D. Thesis, K.N.Toosi University of Tech., IRAN, Sep. 2006.
[14] Z. Qu and D.M. Dawson, Robust tracking control of robot manipulators, IEEE Press, 1996.
[15] J. J. Craig, Adaptive control of mechanical manipulators, Addison Wesley, 1988.